D-STATCOM for Distribution Network Compensation Linked with Wind Generation

Ali M. Eltamaly, Yehia Sayed Mohamed, Abou-Hashema M. El-Sayed, Amer Nasr A. Elghaffar, and Ahmed G. Abo-Khalil

Abstract Wind generation is considered as one of the optimum renewable energy sources due to its more saving running cost, zero-emission, and friendly environment at comparing with the traditional power plants. Using the wind farms with the utility grid can't reach the optimum compensation during any abnormal condition in the power system. Distributed Static Synchronous Compensators (D-STATCOM) is a power electronic control system to be used with the distribution power network for harmonics current elimination, reactive power compensation, voltage regulation, voltage flicker mitigation, and frequency regulation. D-STATCOM provides effective compensation to the unbalance or the nonlinear loads by injecting the required accurate value at the Point of Common Coupling (PCC) depending on the Voltage Source Converter (VSC). This chapter proposes a design procedure of a high-power D-STATCOM with the distribution network linked with the wind generation for enhancing the power system quality. The proposed simulation in this chapter has been done using the MATLAB/Simulink software for distribution voltage control, loadability, and power loss reduction using the D-STATCOM control techniques with the electrical distribution network.

Keywords D-STATCOM · Voltage compensation · Distribution power networks · Power quality

A. M. Eltamaly (✉)
Electrical Engineering Department, Mansoura University, Mansoura, Egypt
e-mail: eltamaly@ksu.edu.sa

Sustainable Energy Technologies Center, King Saud University, Riyadh 11421, Saudi Arabia

K.A. CARE Energy Research and Innovation Center, Riyadh 11451, Saudi Arabia

Y. S. Mohamed · A.-H. M. El-Sayed · A. N. A. Elghaffar
Electrical Engineering Department, Minia University, Minia, Egypt

A. G. Abo-Khalil
Department of Electrical Engineering, College of Engineering, Majmaah University, Almajmaah 11952, Saudi Arabia

Department of Electrical Engineering, College of Engineering, Assuit University, Assuit 71515, Egypt

A. M. Eltamaly et al. (eds.), *Control and Operation of Grid-Connected Wind Energy Systems*, Green Energy and Technology,
https://doi.org/10.1007/978-3-030-64336-2_5

Nomenclature

R	Rotor resistance impedance
U	Output voltage
X1	Stator reactance
X2	Rotor reactance
X_σ	Total reactance rotor and stator
S	Generator slip
Q	Reactive Power
Q_C	The parallel capacitor group
Q_{N-Unit}	Reactive power capacitor compensation capacity
[n]	Assuming actual capacitor investment group
Cp max	Optimal power coefficient
λ	Ratio between the wind speed and the rotor speed
v_w	Wind speed
w	Wind turbine rotational speed
P_m	The extracted mechanical power by the constant pitch
ρ	Air density
C_p	Turbine coefficient
A_r	Area swept by the blades
w_t	The rotational speed
k_{opt}	The unique parameter
L_f	Interfacing inductors
m	The modulation index
w	The system frequency
vA1	Output injection voltage inverter 1
vA2	Output injection voltage inverter 2
i_{A1}	Currents delivered by inverter-1
i_{A2}	Currents delivered by inverter-2
L_0	Mutual inductance
L_{lk}	Leakage inductance
e_{gr}	Equivalent grid voltage
L_{gr}	Equivalent inductance
R_{gr}	Equivalent resistance
v_{gr}	Voltage at the point of common coupling (PCC)
i_{gr}	The current at PCC
v_{A1}	The instantaneous voltage generates by converter-1
v_{A2}	The instantaneous voltage generates by converter-2
v_f	The voltage over filter capacitor c_f

1 Introduction

Doubtless the electrical power system network has a lot of challenges to save the stable system especially with the extension and the increasing of the nonlinear loads. Using the compensation devices for enhancing the system to reach the optimum operation is the solution to save the electrical system in stable condition [1]. The power system quality is affected by the disturbances or any abnormal condition as voltage sag/swell, which directly have an impact on electronic devices or any critical loads causing heating or malfunction of devices and the high cost related to the system shut down. With the extension of the demands of the wind energy to utilize the natural environment and to save the generation running costs, the reactive/voltage control in the distribution system is becoming more important [2]. Wind turbines utilizing the frequency converters are generally fit for controlling the reactive power to zero or potentially of providing or devouring reactive power as indicated by needs, even though this is restricted by the size of the converter [3]. So, it's important to use compatible devices for enhancing the system quality during abnormal conditions [4, 5]. However, unfortunately of using the compensation techniques to finding other bad affection as feeding harmonics by the compensation devices or noncontinuous compensation or finding the inrush current [6]. The system compensation by a fixed shunt capacitor is a simple way, but it's not accurate especially with the fast load variation and with the critical loads. Following the improvement of the power electronics circuits and the advanced methodology, the Flexible AC Transmission Systems (FACTS) devices can solve the power system quality depending on the thyristors technologies [7]. FACTS devices are consisting of the optimum way to operates in fast, accurate compensation techniques, and easy to install with the system for control the voltage profile, damp the power system oscillation [6–8]. Consequently, Custom Power Devices (CPD) are preferred for the electrical power quality improvement due to the lower cost, greater flexibility, and increase of system security [9]. Static Synchronous Compensation (STATCOM) control techniques and Static Var Compensation (SVC) modules are the famous compensation ways of the FACTS families [10–15]. Distributed Static Synchronous Compensators (D-STATCOM) is a shunt compensator device to be installed with the electrical distribution network for voltage control, also it can tackle the power quality issues [16–24]. The D-STATCOM configuration is adaptable enough to abuse multi-usefulness coupling with the power system. Besides, D-STATCOM is a multi-functional gadget that simple to give viable remuneration to the non-direct loads and unbalance stacks by infusing suitable responsive power contingent upon the thyristors for exchanging [21]. Figure 1 shows the streamlined structure to connect the D-STATCOM with the distribution network for improving the PQ. There are many designs of the D-STATCOM multilevel inverter control as Cascaded H-Bridge [22] and Diode-Clamped [23]. However, using a new control technique with the D-STATCOM topology by adding one more converter with the D-STATCOM to increase the voltage source converter power. This chapter discusses the importance of using the D-STATCOM with the distribution system for voltage control depending

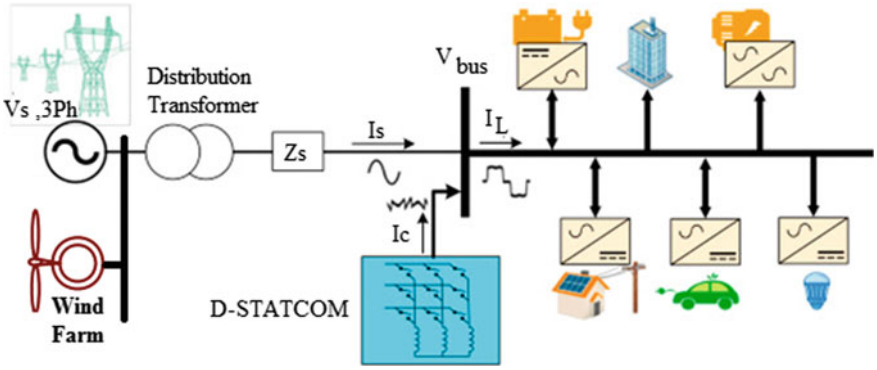

Fig. 1 D-STATCOM for PQ control

on the Voltage Source Converter (VSC) for the optimum power quality improvement. The proposed analysis in this chapter has been validated with the distribution network to compensate for the voltage on a 25-kV distribution network using the MATLAB/SIMULINK software to shows the voltage compensation during the fault condition in the power system.

2 Wind Generation Output Power

Utilizing the environment renewable sources like the wind can be used for rotating the generator to find free electric power without running cost as comparing with the fossil fuel generation system. By the last simple discussion, Fig. 2 shows the fundamental wind turbine parts which depending upon the transformer to connect with the utility grid [24–30]. Moreover, the typical technique to change over the low- and high-speed conditions and to generate the electric power from mechanical power a gearbox and a generator is required to be synchronized with electric utility network. The gearbox changes the low speed of the turbine rotor to high speed. Notwithstanding some types

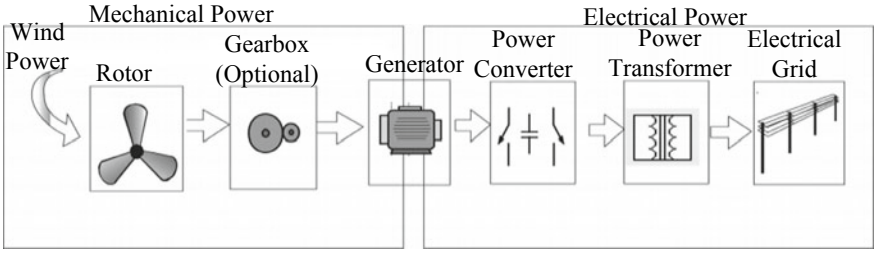

Fig. 2 Main component for WG

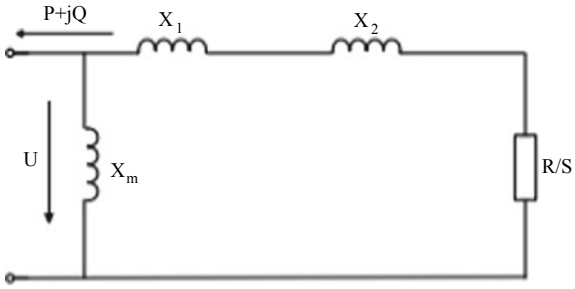

Fig. 3 The equivalent simplification model for WG

of wind turbines like the one use permanent magnet and multipole generator systems are not using gearbox [31]. The wind energy system is considered as precarious for power due to its compelled consistency and irregularity [32]. By using the exchange plans with nearby generating power plants, the power system can disentangle the fluctuations caused by the wind energy systems. At the point when the generated power from the wind is lower than the loads, the primary game plan is used to use standard generation units to cover this shortage of wind power [33]. The wind generation is relying upon the criticism pay through the utility grid, thus, the wind generation can be classified as PQ or PV busbar types in the power stream modeling [34–38]. The coordinated generator circuit can be streamlined to the proportionate circuit as appeared in Fig. 3. Where, the stator resistance can be disregarded, R is the rotor resistance impedance, U is the yield voltage, X1, X2 are the stator, and rotor reactance impedance individually and Xm is the excitation reactance.

Equation (1) shows the total reactance rotor and stator, to uses for calculating the active generated power in Eq. (2).

$$X_\sigma = X_1 + X_2 \tag{1}$$

$$P = \frac{SRU^2}{S^2X_\sigma^2 + R^2} \tag{2}$$

With consideration, S is the generator slip, that is related to Eq. (3) to obtain the reactive power by using Eq. (4).

$$S = R\left(U^2 - \sqrt{U^4 - 4X_\sigma^2P^2}\right)/2PX_\sigma^2 \tag{3}$$

$$Q = \left[R^2 + X_\sigma(X_m + X_\sigma)S^2\right]/SRX_m \tag{4}$$

There are various methods when choosing the reactive power compensation system inside the WG gatherer design, the parallel shunt capacitors with the WG can compensate for the reactive power [39–42]. Which able to calculates by the below equation number (5) to find the total required capacitor group value Q_C from Eq. (6).

$$\mathrm{Cos}(\varnothing) = \mathrm{P}/\sqrt{\mathrm{P}^2(\mathrm{Q_C} - \mathrm{Q})^2} \tag{5}$$

$$\mathrm{Q} = \mathrm{P}\left[\sqrt{\frac{1}{(\mathrm{Cos}(\varnothing 1))^2} - 1} - \sqrt{\frac{1}{(\mathrm{Cos}(\varnothing 2))^2} - 1}\right] \tag{6}$$

Chosen the compatible and prober way should follow the prerequisites of the WG plant. Further things for thought may incorporate voltage impediments, especially during the switching of shunt capacitors, power quality necessities, for example, glint during fire up or cut-in, harmonics, and so forth [43, 44]. By expecting the real capacitor speculation bunch is [n], and the receptive power capacitor pay limit is Q_(N-Unit), which mimics at the evaluated voltage, which can use to generate the WG reactive power from Eq. (8).

$$[\mathrm{n}] = \mathrm{Q_C}/\mathrm{Q_{N-Unit}} \tag{7}$$

$$\mathrm{Q}' = \mathrm{Q_C} - \mathrm{Q} \tag{8}$$

The controller used for WG speed control essential function is the Maximum Power Point Tracking (MPPT) of the available power in the wind. An expanding number of bigger WGs (starting from1 MW and more) are created with a functioning slow down power control component. Actually, the dynamic slow down turbines take after pitch-controlled turbines since they have pitch capable blades. To get a sensibly huge force (turning power) at low wind speeds, the WG will ordinarily be customized to pitch their blades a lot of like a pitch-controlled wind turbine at low wind speeds. Regularly they utilize just a couple of fixed advances depending on the wind speed. At the point when the turbine arrives at its evaluated power, nonetheless, it will see a significant distinction from the pitch-controlled wind turbines: If the generator is going to be over-burden, the turbine will contribute its blades the other way from what a pitch-controlled WG does. As such, it will build the approach of the rotor blades to cause the blades to go into a more profound slow down, in this manner squandering the overabundance energy in the wind [45]. One of the active stalls of a functioning slowdown is that one can control the active power more precisely than with passive stall, to abstain from overshooting the appraised power of the turbine toward the start of a whirlwind. Another preferred position is that the WG can be run precisely at the evaluated power of the machine at all high wind speeds [43–45]. Figure 4 shows the variable wind speed [43]. Where, (λ) is the tip-speed to simulate the ratio between the wind speed and the rotor speed as shown in Eq. (9).

$$\lambda = \frac{\mathrm{R_p w}}{\mathrm{v_m}} \tag{9}$$

with considering, is the wind speed represented by $\mathrm{v_w}$ and the WG speed is *w* [46]. Hence, the extracted mechanical power by the constant pitch can be calculated from

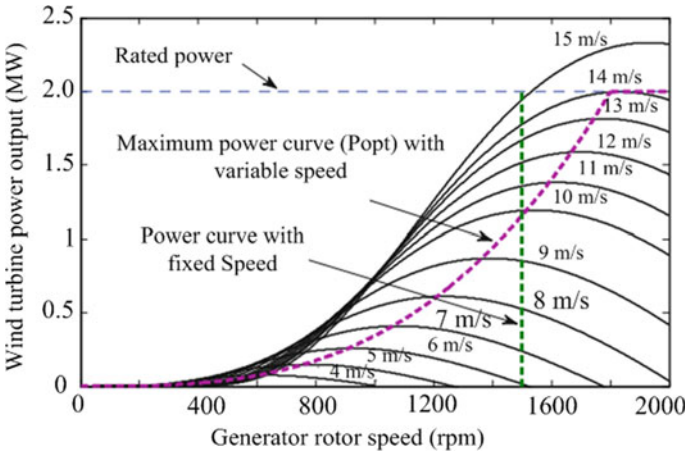

Fig. 4 Wind generation output power during fixed and variable wind speed

the below Eq. (10):

$$P_m = \frac{1}{2}.\rho A_r v_w^3.C_p(\lambda) \tag{10}$$

where; ρ is the air density is presented by ρ, the turbine coefficient presented by C_p and the area swept by the blades can simulate by A_r. The wind velocity V1, V2 are presented for WG control curve as shown in Fig. 5. With a note, at the WG

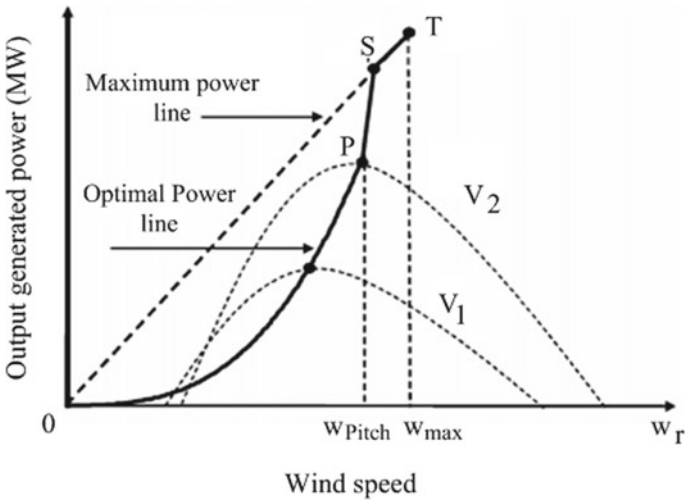

Fig. 5 WG power control curve

operates at optimal power coefficient (Cp max) in this simulation, at each velocity, there is one maximum power capture point [47]. Moreover, an individual optimal power available for the WG speed by using the below Eq. (11).

$$P_{opt} = k_{opt} w_T^3 \tag{11}$$

where, w_t is the rotational speed and k_{opt} is the unique parameter.

3 D-STATCOM Control Strategies

D-STATCOM control techniques are designed to link with the three-phase power system by three-phase stacks as shown in Fig. 1. The D-STATCOM is a shunt connected custom power device depending on the Direct Current (DC) energy storage for injection of the voltage through the coupling transformer under control by the VSC converts and the output filter. The point of adding the VSC to convert the DC stockpiling batteries voltage to the decent three-phase AC yield voltages. The created voltages are in-phase and interconnected with the utility grid through a coupling transformer. D-STATCOM legitimate yield setting of the phase angle and the voltage greatness permits successful control of active and reactive power flow between the D-STATCOM and the utility distribution system [48]. The three-phase loads may be of various sorts like lagging power factor, unbalance, linear or nonlinear loads, and joined among linear and nonlinear loads. However, to reduce the swiping in the compensating current, it requires to use the interfacing inductors (L_f) at the AC side of the VSC. The operation characteristics of the D-STATCOM can be justified depending on the dc-link capacitor, equivalent transformer. An insulated-gate bipolar transistor (IGBT)-based VSC, and filter resistance, and filter inductance, and the utility grid as a three-phase source. Figure 6 shows the equivalent D-STATCOM circuit, which can use to find the combination of the PCC voltage and the inverter-generated voltage for system compensation.

The simplified equation for phase (A), phase (B), and phase (C) can find from Eqs. (12), (13), (14), respectively.

$$R_s i_a + L_s \left[\frac{di_a}{dt}\right] = V_{Pa} - V_{ca} \tag{12}$$

$$R_s i_b + L_s \left[\frac{di_b}{dt}\right] = V_{Pb} - V_{cb} \tag{13}$$

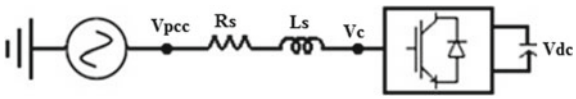

Fig. 6 D-STATCOM equivalent simplified circuit

$$R_s i_c + L_s\left[\frac{di_c}{dt}\right] = V_{Pc} - V_{cc} \tag{14}$$

By transforming the equations to obtain the below equations, with considering m is the modulation index, the frequency is w.

$$L_s\left[\frac{di_d}{dt}\right] + R_s i_d = V_{Pd} - mV_{dc}\cos\theta + L_s w_{iq} \tag{15}$$

$$L_s\left[\frac{di_q}{dt}\right] + R_s i_{dq} = V_{Pq} - mV_{dc}\sin\theta - L_s w_{id} \tag{16}$$

where from Eqs. (15) and (16) can be justified as shown in Eq. (17).

$$\frac{d}{dt}\begin{bmatrix} id \\ iq \end{bmatrix} = \begin{pmatrix} -R_s/L_s & w \\ -w & -R_s/L_s \end{pmatrix}\begin{bmatrix} id \\ iq \end{bmatrix} + \frac{1}{L_s}\begin{pmatrix} V_{pd} - V_{cd} \\ V_{pq} + V_{cq} \end{pmatrix} \tag{17}$$

The simplified equations are simplified by ignoring the voltage harmonics as shown in the following.

$$m.V_{dc}\cos\theta = V_{cd} \tag{18}$$

$$m.V_{dc}\sin\theta = V_{cq} \tag{19}$$

By considering the inverter is a lossless circuit, so the instantaneous power can be found by the power balance theory at the ac-dc terminal to find as shown in Eq. (20) and the dc side circuit can find as shown in Eq. (21).

$$V_{dc}.i_{dc} = \frac{3}{2}(V_{cd}.id + V_{cq}.iq) \tag{20}$$

$$i_{dc} = C.\frac{d(V_{cd})}{dt} = \frac{3}{2}.m.(id.\cos\theta - iq.\sin\theta) \tag{21}$$

By combining Eq. (17) and Eq. (21)

$$\frac{d}{dt}\begin{pmatrix} i_d \\ i_q \\ V_{dc} \end{pmatrix} = F\begin{pmatrix} i_d \\ i_q \\ V_{dc} \end{pmatrix} - \frac{1}{Ls}\begin{pmatrix} i_d \\ i_q \\ V_{dc} \end{pmatrix}$$

where, F is given as:

$$\begin{pmatrix} -R_s/L_s & w & \frac{-m}{L_s}\cos\theta \\ -w & -R_s/L_s & \frac{m}{L_s}\sin\theta \\ \frac{3}{2}\frac{m}{c}\cos\theta & \frac{-3}{2}\frac{m}{c}\sin\theta & 0 \end{pmatrix} \tag{22}$$

At this point, to illustrate the active and reactive power for D-STATCOM compensation, it can simplify by the below Eqs. (23), (24), respectively.

$$P = V_{pd.id} + V_{pd.iq} = V_{pd.id} = V_{pd.id} \tag{23}$$

$$q = V_{pq.id} - V_{pq.iq} = -V_{pd.iq} = -V_{pd.iq} \tag{24}$$

Finally, the D-STATCOM module operates to compensate the system depending on controlling of *id*, *iq* as shown in Eq. (23) for active power injection and Eq. (24) for the reactive power injection to the distribution busbar.

4 D-STATCOM Characteristic Logic

Depending on the coupling of magnetic elements for the parallelization of standard two-level or three-level inverters using the D-STATCOM dual-converter configuration can be created to increase the VSC output power as shown in Fig. 7 for the dual-converter with common DC link and Fig. 8 for the dual-converter with isolated DC link [49, 50]. According to the coupling between the two converters, an equal

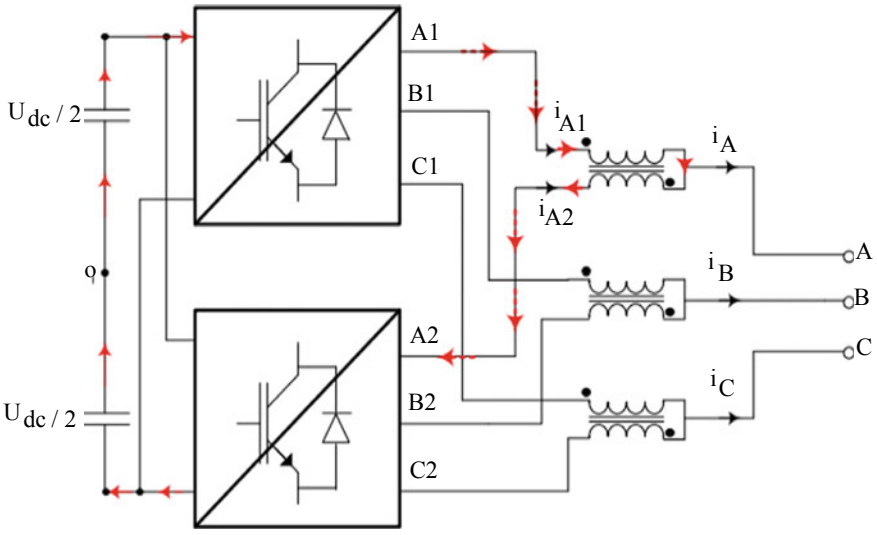

Fig. 7 D-STATCOM Configurations using the dual-converter topology with a common DC link

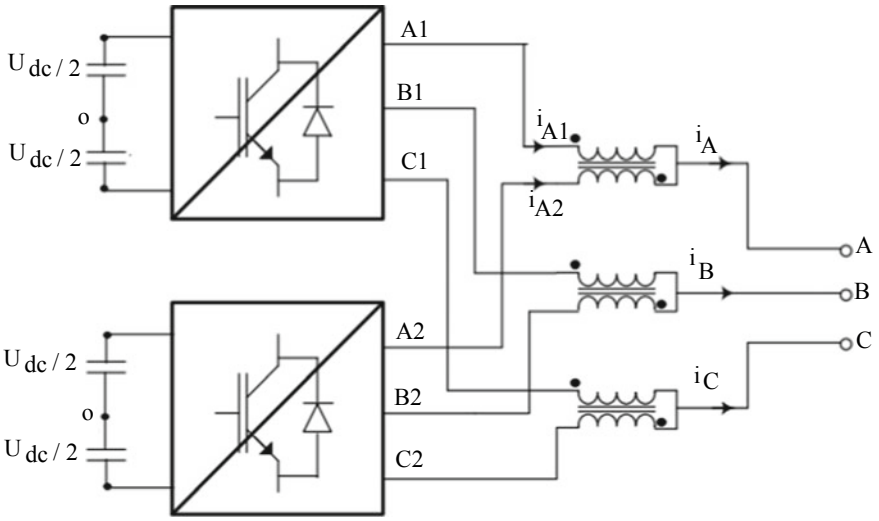

Fig. 8 D-STATCOM the dual-converter design with separated DC link

current will flow from both converters, which can be known as a parallel interleaved VSC [51]. The harmonic injection can be significantly reduced by the interleaved carrier signal of both SVCs, which is phase-shifted by 180° [51–53]. With notes, there is a potential difference between the output injection voltage V_{A1} and V_{A2} due to carriers are interleaved.

The circulating current is depressed by the effection of the DC links which is described in Figs. 7 and 8. Where VSC contains two parallel parts of three-phase converters. The parallelization of inverter phases is accomplished by the methods for two neighboring coils that are attractively connected. Ignoring copper losses, the mutual induction between the coupled coils can be portrayed by the equivalent circuit for Phase-A in Fig. 9, where the currents delivered by each inverter is i_{A1} and i_{A2}, to express as a function of common-mode current i_{mc} and differential-mode current i_{md} (circulating current) as shown in Eqs. (25) and (26).

$$i_{A1} = \frac{i_{mc}}{2} + i_{md} \tag{25}$$

$$i_{A2} = \frac{i_{mc}}{2} - i_{md} \tag{26}$$

With a note, the two inductors in the same phase are the same number of turns and arranged on the same ferromagnetic core [51]. The mutual inductance L_0 and the leakage inductance L_{lk} can be expressed in function of the self-inductance, where k expresses the coupling factor between the coils that can equalize "1" at the two coils symmetrically, to be used as shown in Eqs. (27) and (28):

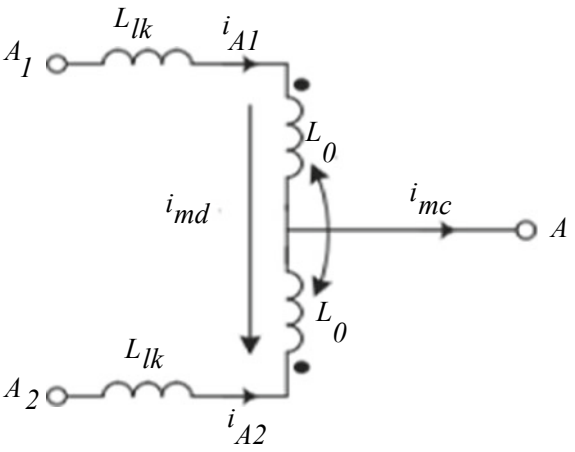

Fig. 9 D-STATCOM equivalent circuit

$$L_0 = \mathrm{kL} \tag{27}$$

$$L_{lk} = (1 - \mathrm{k})\mathrm{L} \tag{28}$$

The two coils are connecting to cancel the induced magnetic field as shown in the polarity points for both coils as shown in Fig. 9, to find the difference potential between the two points A1 and A2 as describes in Eq. (29).

$$v_{A1o} - v_{A2o} = (2L_{lk} + 4L_0)\frac{di_{md}}{dt} \tag{29}$$

where, the inductive reactance $L_0\omega$ seen by differential-mode currents as the quarter value of the impedance. The circulating currents can be decreased by the separation of DC links as shown in the equivalent circuit diagram in Fig. 10. DC link isolates to repress the zero-sequence track, and zero-sequence circulating current to be no longer among the two converters [51].

LCL filter is the common coupling part between the electrical system and D-STATCOM. Figure 11 shows the equivalent circuit for single-phase D-STATCOM with an LCL filter with neglecting the copper losses. Where, e_{gr} is the equivalent grid voltage, L_{gr} is the equivalent inductance, v_{gr} is the voltage at PCC point, R_{gr} is the total equivalent resistance, and i_{gr} is the current at PCC. Equations (30) to (34) shows the differential equations for the filter dynamics.

$$v_{A1} = L_{lk}\frac{di_{A1}}{dt} + L_0\frac{di_{A1}}{dt} - L_0\frac{di_{A2}}{dt} + v_A \tag{30}$$

$$v_{A2} = L_{lk}\frac{di_{A2}}{dt} + L_0\frac{di_{A2}}{dt} - L_0\frac{di_{A1}}{dt} + v_A \tag{31}$$

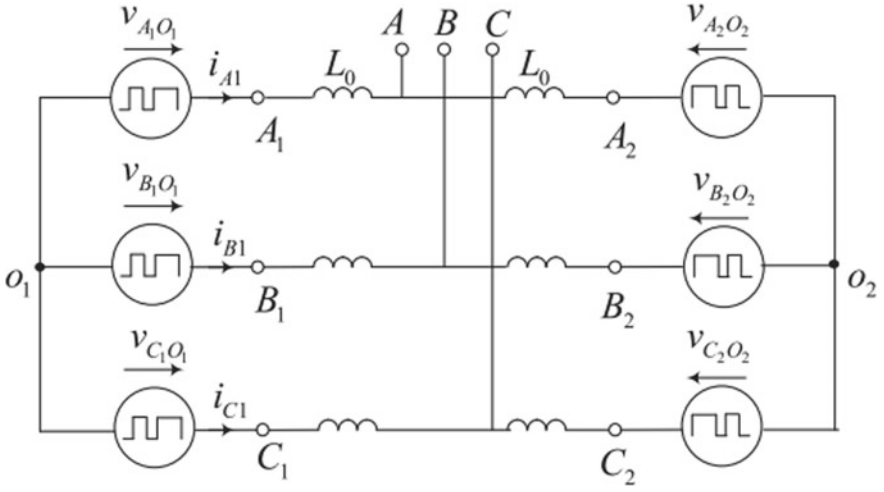

Fig. 10 Isolated DC link for D-STATCOM dual-converter

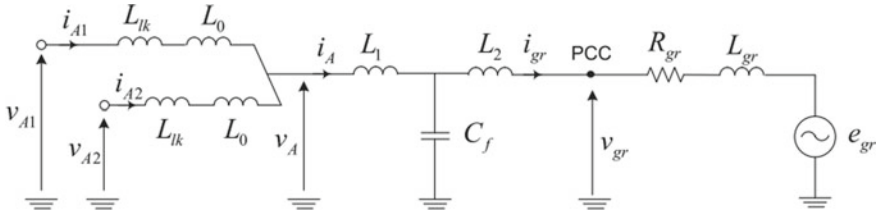

Fig. 11 Single-phase D-STATCOM equivalent circuit with LCL filter

$$v_A = L_1 \frac{di_A}{dt} + v_f \tag{32}$$

$$v_f = (L_2 + L_{gr}) \frac{di_{gr}}{dt} + R_{gr} i_{gr} + e_{gr} \tag{33}$$

$$\frac{v_{A1} + v_{A2}}{2} = \frac{L_{lk}}{2} \frac{di_A}{dt} + v_A \tag{34}$$

where, v_{A1} is the instantaneous voltage generates by converter-1, v_{A2} is the instantaneous voltage generates by converter-2, and v_f is the voltage over the filter capacitor c_f.

The common-mode voltage is defined by:

$$v_{mc} = \frac{v_{A1} + v_{A2}}{2} \tag{35}$$

The thunderous frequency is picked lower than the tweak frequency of the double converter, and the shunt capacitors of the LCL filter ought to be picked as little as conceivable because they draw receptive power, this part is fully discussed in [51].

5 D-STATCOM Simulation

D-STATCOM control techniques are used with the distribution power network to manage voltage during abnormal conditions. Figure 12 shows an example of an electrical system contains three busbars, variable loads linked at busbar-B2 and busbar-B3, two feeder lines (21 and 2 km) to fed the lads, and D-STATCOM module linked with 25 kV system. The shunt capacitor bank is used for power factor correction at busbar-B2. The variable loads at busbar-B3 are operating through a step-down transformer 25 kV/600 V to a plant retaining constantly evolving currents, in this way creating voltage flicker. At 5.0 Hz frequency, can regulate the variable magnitude of the load current which obvious the apparent power between 1.0 and 5.2 MVA, with saving the power factor at 0.9 lag. The load variation in this simulation will allow us to describe the capacity of the D-STATCOM to compensate voltage which can add capacitance value or reactance value depending on the required action as shown in Fig. 13. The D-STATCOM is connected with busbar-B3 to compensate for the reactive power by generates the in-phase voltage by a voltage source PWM inverter with the utility grid [54].

5.1 D-STATCOM Operation Characteristics

During this simulation, the load is starting a constant value to observe the D-STATCOM response to step changes in source voltage [55]. With notes, the modulation of the variable load is not in service, which depending on the Time-on and Time-off = [0.15 1] *100 > simulation stop time. The voltage source block is adjusted to simulate the internal voltage of 25.0 kV; however, the voltage is starting at 1.077pu to keep the floating injection by the D-STATCOM at busbar-3 by 1.0 pu as comparing

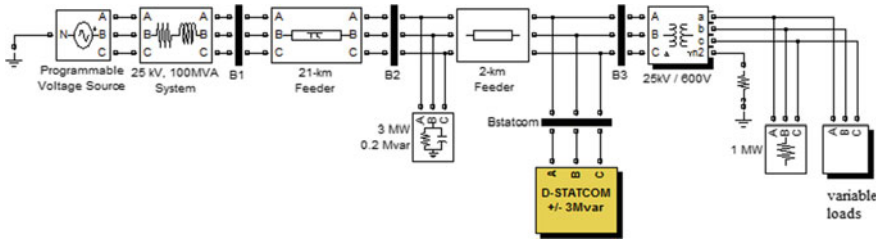

Fig. 12 D-STATCOM simulation with distribution network

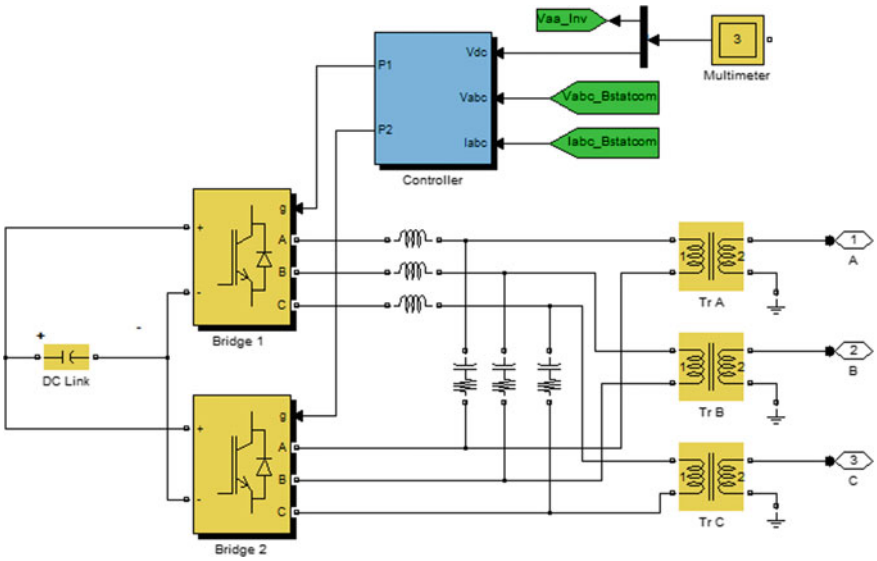

Fig. 13 D-STATCOM design with 2 inverters

with the reference value 1.0 pu. The D-STATCOM is programmed to operates by three steps at 0.2 s, 0.3 s, and 0.4 s for increasing the voltage source by 6.0% or decrease the voltage by 6.0% and return to be 1.077 pu. At 0.15second, the transient happened in the system at so the D-STATCOM will start to compensate the system at 0.2 s to increase the voltage by 6% by absorbing the system reactive power by Q = + 2.7 Mvar as shown in Fig. 14. At time = 0.3 s the voltage source is decreased by 6.0% from the corresponding voltage to reach the reactive compensation 0.0 Mvar. Additionally, the D-STATCOM is required to compensate the system voltage to reach the reference value 1.0 p.u to change the reactive compensation from inductive to capacitive between -2.8 Mvar and 2.7 Mvar, as shown in Fig. 15 for the PWM inverter 0.56 p.u to 0.9 which corresponds to a proportional increase in inverter voltage [54, 55]. Figure 16 shows the fast reversing of reactive power at one cycle by the D-STATCOM current.

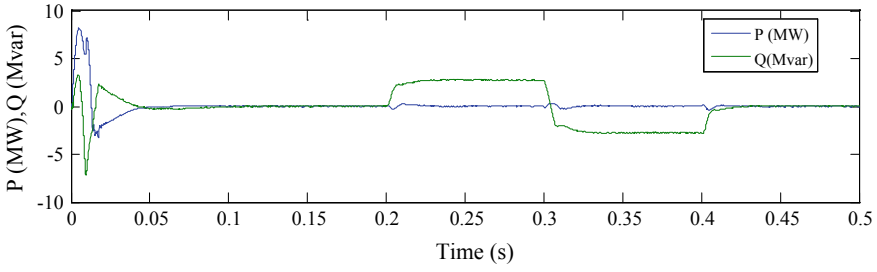

Fig. 14 D-STATCOM consumes the system reactive power (Q = + 2.7 Mvar)

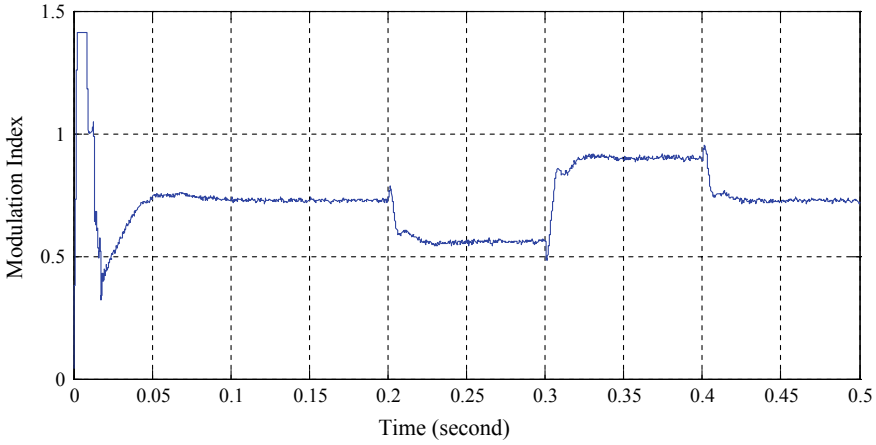

Fig. 15 D-STATCOM performed by PWM from 0.56 p.u to 0.9

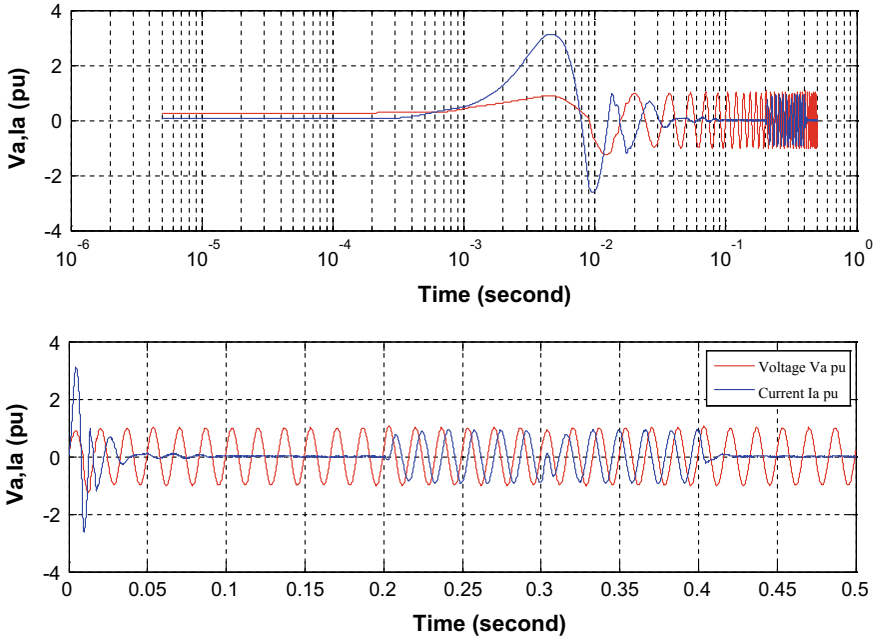

Fig. 16 Shows the fast reversing of reactive power at one cycle by the D-STATCOM current

5.2 Mitigation of Voltage Flicker

To simulate the operation characteristics of D-STATCOM for voltage compensation, it needs to variate the loads' value. By changing the "Time Variation of" In the Programmable Voltage Source block menu parameter to "None," with set the Modulation Timing Parameter in the Variable Load block menu to [Ton Toff] = [0.15 1] (without 100-multiplication factor). Also, change the "Mode of operation" parameter to "Q regulation" in the D-STATCOM control part, and set the reference reactive power Q value as zero. In this mode, D-STATCOM compensation techniques are not affecting the voltage. After running the system and check the operation for D-STATCOM as shown in Fig. 17 to verify the active power P and reactive power Q at busbar-B3, moreover, busbar-B1, and B3 voltages are simulated in Fig. 18. In another hand, without adding the D-STATCOM, the voltage at busbar-B3 will vary in range (0.96:1.04) pu [54, 55]. But, after adding the D-STATCOM control techniques, the voltage at busbar-B3 is reduced to ±0.7%. In Fig. 19, D-STATCOM compensates the voltage by injecting a reactive current which formed at 5.0 Hz as depending on

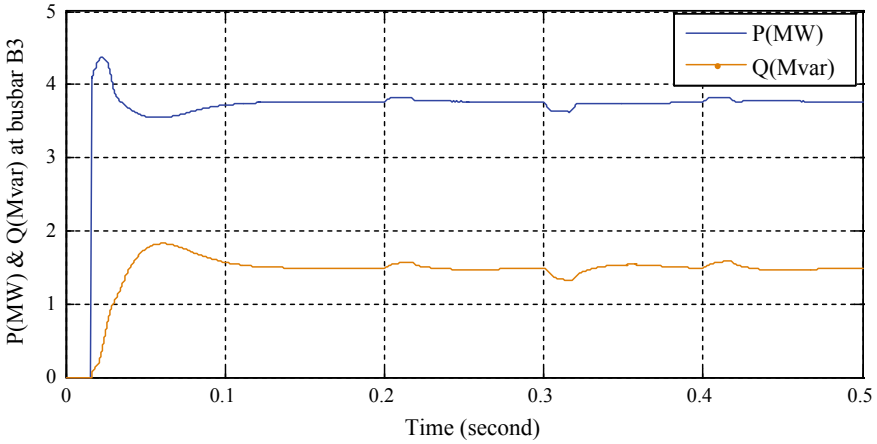

Fig. 17 For variations of P and Q at busbar-B3

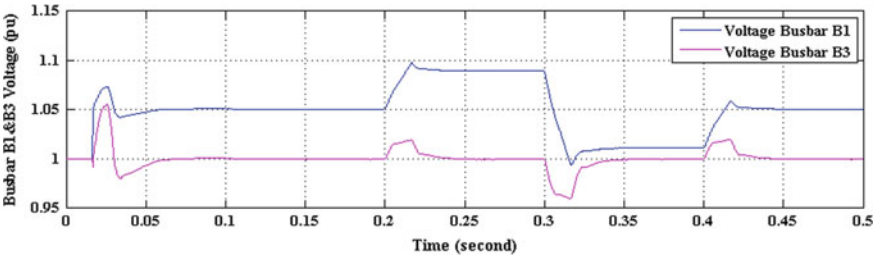

Fig. 18 Voltage value at busbar-B1 and busbar-B3

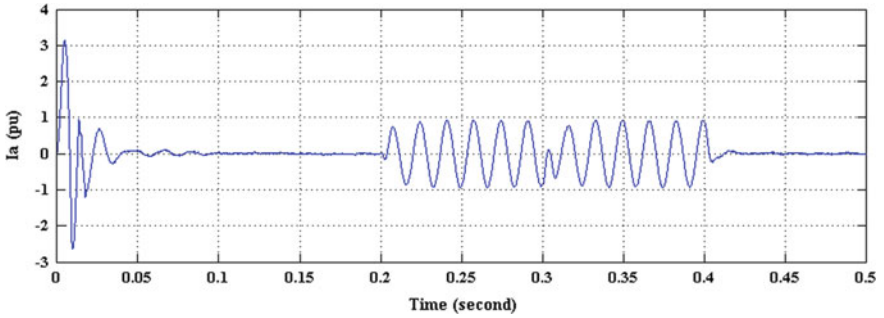

Fig. 19 D-STATCOM injection reactive current modulated at 5.0 Hz

the varying between capacitive and reactive related to the required compensation at the under/over voltage, respectively.

6 Conclusion

The blend of renewable energy sources like solar or wind energy to the electrical grid affects stability and system quality. The power system designers have to ensure a stable system and their services to retain the system in the stable region at any abnormal condition in the system. Using D-STATCOM techniques with the distribution network can achieve for enhancing the PQ. Adding the battery and the capacitor bank are used as the DC busbar in the design of D-STATCOM. In this chapter, the D-STATCOM has been demonstrated for improving power system quality during various operational events. The abnormal conditions in the distribution system as the tripping/reclosing of distribution feeder, energizing high-power transformer, switching ON/OFF of capacitor, or inductive-resistive loads. This chapter investigated one of the FACTS modules of D-STATCOM to be linked with the distribution network as a fully inductive/capacitive load as required for compensation under the support by the battery bank to be used for PQ enhancement. Finally, in this chapter, the simulation analysis was carried by MATLAB/Simulink software to discusses the operation steps of D-STATCOM to reach the optimum compensation for saving the voltage in the required stable region.

Acknowledgements The authors wish to acknowledge Alfanar Company, Saudi Arabia for supporting to complete this research, especially thanks to Mr. Amer Abdullah Alajmi (General Manager, Alfanar Engineering Service, Saudi Arabia) and Mr. Osama Morsy (Executive Manager, Alfanar Testing and Commissioning, Saudi Arabia).

References

1. Eltamaly AM et al (2020) Adaptive static synchronous compensation techniques with the transmission system for optimum voltage control. Ain Shams Eng J. https://doi.org/10.1016/j.asej.2019.06.002
2. Eltamaly AM, Elghaffar ANA et al (2018) Enhancement of power system quality using PI control technique with DVR for mitigation voltage sag. In: 2018 Twentieth international middle east power systems conference (MEPCON), Cairo, Egypt; 12/2018. https://doi.org/10.1109/MEPCON.2018.8635221
3. Eltamaly AM, Sayed Y, Abou-Hashema A, Elghaffar ANA (2020) Small-scale wind distributed generation with the power distribution network for power quality control. In: Emerging technologies and their applications in the service of sustainable development in the Arab world. 21–23 June 2020
4. Chen Z et al (2009) A review of the state of the art of power electronics for wind turbines. IEEE Trans Power Electron 24(8) (2009)
5. Ackermann T (2005) Wind power in power systems. Wiley, Book
6. Sayed Y, Abou-Hashema M, Elghaffar ANA, Eltamaly AM (2019) Multi-shunt VAR compensation SVC and STATCOM for enhance the power system quality. J Electr Eng 19
7. Brito MEC et al Adjustable VAr compensator with losses reduction in the electric System. Elec Eng J https://doi.org/10.1007/s00202-018-0692-x
8. Bindumol EK (2017) Impact of D-STATCOM on voltage stability in radial distribution system. In: International conference on energy, communication, data analytics and soft computing (ICECDS-2017)
9. Mehrdad Ahmadi Kamarposhti and Mostafa Alinezhad (2010) Comparison of SVC and STATCOM in static voltage stability margin enhancement. Int J Electr Electron Eng 4:5
10. Duarte SN et al (2020) Control algorithm for DSTATCOM to compensate consumer-generated negative and zero sequence voltage unbalance. Int J Electr Power Energy Syst 120. https://doi.org/10.1016/j.ijepes.2020.105957
11. Elghaffar ANA, Eltamaly AM, Sayed Y, Elsayed AHM (2018) Advanced control techniques for enhance the power system stability at OOS condition. Energy Sci J
12. Eltamaly AM, Mohamed YS, El-Sayed AHM, Elghaffar ANA (2019) Impact of distributed generation (DG) on the distribution system network. Ann Fac Eng Hunedoara 17(1):165–170
13. Eltamaly AM, Sayed Y, El-Sayed AHM, Elghaffar ANA (2018) Optimum power flow analysis by Newton raphson method, a case study. Ann Fac Eng Hunedoara 16(4):51–58s
14. Eltamaly AM, Sayed Y, El-Sayed AHM, Elghaffar ANA (2018) Mitigation voltage sag using dvr with power distribution networks for enhancing the power system quality. IJEEAS J 2600–7495
15. Elghaffar AA, Eltamaly A, Sayed Y, El-Sayed A-H (2018) Enhancement of power system quality using static synchronous compensation (STATCOM). EISSN, IJMEC, pp 2305–2543
16. Kamalakannan C et al (eds) Power electronics and renewable energy systems, lecture notes in electrical engineering 326. Chapter 40, Improvement of power quality in distribution system Using D-STATCOM. https://doi.org/10.1007/978-81-322-2119-7_40
17. Eltamaly AM, Sayed Y, Mustafa AH, Elghaffar ANA (2018) Multi-control module static VAR compensation techniques for enhancement of power system quality. Ann Fac Eng Hunedoara 16(3):47–51
18. Elghaffar NA, Eltamaly AM, Sayed Y, El-Sayed AHM (2018) The effectiveness of dynamic voltage restorer with the distribution networks for voltage sag compensation. Int J Smart Electr Eng 7(02):61–67
19. Eltamaly AM (2009) Harmonics reduction techniques in renewable energy interfacing converters. Renew Energy Intechweb
20. Eltamaly AM (2012) Novel third harmonic current injection technique for harmonic reduction of controlled converters. J Power Electron 12(6):925–934
21. Vural AM (2016) Self-capacitor voltage balancing method for optimally hybrid modulated cascaded H-bridge D-STATCOM. IET Power Electron 9:2731–2740

22. Gawande SP, Ramteke MR (2014) Three-level NPC inverter based new DSTATCOM topologies and their performance evaluation for load compensation. Int J Electr Power Energy Syst 61:576–584
23. Yang J et al (2013) The impact of distributed wind power generation on voltage stability in distribution systems. In: (APPEEC) conference
24. Eltamaly AM, Mohamed YS, El-Sayed AHM, Elghaffar ANA (2019) Reliability/security of distribution system network under supporting by distributed generation. Insight-Energy Sci 2(1):1–14
25. Eltamaly AM, Alolah AI, Abdel-Rahman MH (2011) Improved simulation strategy for DFIG in wind energy applications. Int Rev Model Simul 4(2)
26. Eltamaly AM, Khan AA (2011) Investigation of DC link capacitor failures in DFIG based wind energy conversion system. Trends Electr Eng 1, 12–21
27. Eltamaly AM (2012) A novel harmonic reduction technique for controlled converter by third harmonic current injection. Electr Power Syst Res 91, 104–112
28. Eltamaly AM, Alolah AI, Farh HM, Arman H (2013) Maximum power extraction from utility-interfaced wind turbines. New Dev Renew Energy 159–192
29. Eltamaly AM, Mohamed MA (2014) A novel design and optimization software for autonomous PV/wind/battery hybrid power systems. Math Probl Eng 2014
30. Eltamaly AM, Al-Shamma'a AA (2016) Optimal configuration for isolated hybrid renewable energy systems. J Renew Sustain Energy 8(4):045502
31. Narasimha Raju VSN et al (2019) A novel approach for reactive power compensation in hybrid wind-battery system using distribution static compensator. Int J Hydrog Energy 44(51):27907–27920, 22 Oct 2019. https://doi.org/10.1016/j.ijhydene.2019.08.261
32. Eltamaly AM, Farh HM (2015) Smart maximum power extraction for wind energy systems. In: 2015 IEEE international conference on smart energy grid engineering (SEGE), pp 1–6. IEEE
33. Shouxiang W et al (2006) Power flow analysis of distribution network containing wind power generators. Power Syst Technol 30:42–45
34. Eltamaly AM, Elghaffar ANA (2017) Load flow analysis by gauss-seidel method; a survey. Int J Mechatron, Electr Comput Technol (IJMEC), PISSN (2017), 2411–6173
35. Khaled U, Eltamaly AM, Beroual A (2017) Optimal power flow using particle swarm optimization of renewable hybrid distributed generation. Energies 10(7):1013
36. Eltamaly AM, Sayed Y, Elghaffar ANA (2017) Power flow control for distribution generator in egypt using facts devices. Acta Tech Corviniensis-Bull Eng 10(2)
37. Eltamaly AM, Al-Saud MS (2018) Nested multi-objective PSO for optimal allocation and sizing of renewable energy distributed generation. J Renew Sustain Energy 10(3):035302
38. Eltamaly AM, Elghaffar ANA (2017) Modeling of distance protection logic for out-of-step condition in power system. Electr Eng 11
39. Jamil E et al (2019) Power quality improvement of distribution system with photovoltaic and permanent magnet synchronous generator based renewable energy farm using static synchronous compensator. Sustain Energy Technol Assess 35:98–116. https://doi.org/10.1016/j.seta.2019.06.006
40. Eltamaly AM (2007) Modeling of wind turbine driving permanent magnet generator with maximum power point tracking system. J King Saud Univ-Eng Sci 19(2):223–236
41. Eltamaly AM (2017) Harmonic injection scheme for harmonic reduction of three-phase controlled converters. IET Power Electron 11(1):110–119
42. Eltamaly AM, Alolah AI, Abdel-Rahman MH (2010) Modified DFIG control strategy for wind energy applications. In: SPEEDAM 2010, pp 653–658. IEEE
43. Li L et al (2015) Maximum power point tracking of wind turbine based on optimal power curve detection under variable wind speed. Int Conf RPG 2015. https://doi.org/10.1049/cp.2015.0492
44. Camm EH, Behnke MR et al (2009) Reactive power compensation for wind power plants. IEEE Power Energy Soc Gen Meet, Canda. https://doi.org/10.1109/PES.2009.5275328
45. Mihet-Popa L et al (2010) Dynamic modeling, simulation and control strategies for 2 Mw wind generating systems. Int Rev Model Simul

46. El-Tamaly AM, El-Tamaly HH, Cengelci E, Enjeti PN, Muljadi E (1999) Low cost PWM converter for utility interface of variable speed wind turbine generators. In: 1999 Conference proceedings (Cat. No. 99CH36285) APEC'99. Fourteenth annual applied power electronics conference and exposition, vol 2, pp 889–895. IEEE
47. Rana AJ et al (2016) Application of unit template algorithm for voltage sag mitigation in distribution line using D-STATCOM. In: 2016 International conference on energy efficient technologies for sustainability (ICEETS), India. https://doi.org/10.1109/ICEETS.2016.7583849
48. Laka A, Barrena JA, Zabalza JC, Vidal R (2013) Parallelization of two three-phase converters by using coupled inductors built on a single magnetic. Prz Elektotechnicy 89:194–198
49. Laka A, Barrena JA, Zabalza JC, Vidal R, Izurza-Moreno P (2014) Isolated double-twin VSC topology using three-phase IPTs for high-power applications. IEEE Trans Power Electron 29(57):61–69
50. Mehouachi I et al (2019) Design of a high-power D-STATCOM based on the isolated dual-converter topology. Electr Power Energy Syst 106:401–410
51. Matsui K, Murai Y, Watanabe M, Kaneko M, Ueda F (1993) A pulse width-modulated inverter with parallel connected transistors using current-sharing reactors. IEEE Trans Power Electron 8:186–191
52. Zhang D, Wang F, Burgos R, Lai R, Thacker T, Boroyevich D (2008) Interleaving impact on harmonic current in dc and ac passive components of paralleled three-phase voltage-source converters. In: 23th annual IEEE applied power electronics conference and exposition
53. Farh HM, Eltamaly AM (2013) Fuzzy logic control of wind energy conversion system. J Renew Sustain Energy 5(2):023125
54. Singh B et al (2018) GA for enhancement of system performance by DG incorporated with D-STATCOM in distribution power networks. J Electr Syst Inf Technol 5:388–426. https://doi.org/10.1016/j.jesit.2018.02.005
55. Mahela OP et al (2016) Power quality improvement in distribution network using DSTATCOM with battery energy storage system. Electr Power Energy Syst 83, 229–240. https://doi.org/10.1016/j.ijepes.2016.04.011